

# Premenopausal Women with a Distal Radial Fracture Have Deteriorated Trabecular Bone Density and Morphology Compared with Controls without a Fracture

Tamara D. Rozental, MD, Laura N. Deschamps, BA, Alexander Taylor, BA, Brandon Earp, MD, David Zurakowski, PhD, Charles S. Day, MD, and Mary L. Bouxsein, PhD

*Investigation performed at the Departments of Orthopaedic Surgery, Harvard Medical School, Beth Israel Deaconess Medical Center, and Brigham and Women's Hospital, Boston; the Department of Medicine, Endocrine Division, Massachusetts General Hospital, Boston; and the Department of Anesthesiology, Harvard Medical School, Boston Children's Hospital, Boston, Massachusetts*

**Background:** Measurement of bone mineral density by dual x-ray absorptiometry combined with clinical risk factors is currently the gold standard in diagnosing osteoporosis. Advanced imaging has shown that older patients with fragility fractures have poor bone microarchitecture, often independent of low bone mineral density. We hypothesized that premenopausal women with a fracture of the distal end of the radius have similar bone mineral density but altered bone microarchitecture compared with control subjects without a fracture.

**Methods:** Forty premenopausal women with a recent distal radial fracture were prospectively recruited and matched with eighty control subjects without a fracture. Primary outcome variables included trabecular and cortical microarchitecture at the distal end of the radius and tibia by high-resolution peripheral quantitative computed tomography. Bone mineral density at the wrist, hip, and lumbar spine was also measured by dual x-ray absorptiometry.

**Results:** The fracture and control groups did not differ with regard to age, race, or body mass index. Bone mineral density was similar at the femoral neck, lumbar spine, and distal one-third of the radius, but tended to be lower in the fracture group at the hip and ultradistal part of the radius ( $p = 0.06$ ). Trabecular microarchitecture was deteriorated in the fracture group compared with the control group at both the distal end of the radius and distal end of the tibia. At the distal end of the radius, the fracture group had lower total density and lower trabecular density, number, and thickness compared with the control group ( $-6\%$  to  $-14\%$ ;  $p < 0.05$  for all). At the distal end of the tibia, total density, trabecular density, trabecular thickness, and cortical thickness were lower in the fracture group than in the control group ( $-7\%$  to  $-14\%$ ;  $p < 0.01$ ). Conditional logistic regression showed that trabecular density, thickness, separation, and distribution of trabecular separation remained significantly associated with fracture after adjustment for age and ultradistal radial bone mineral density (adjusted odds ratios [OR]: 2.01 to 2.98;  $p < 0.05$ ). At the tibia, total density, trabecular density, thickness, cortical area, and cortical thickness remained significantly associated with fracture after adjustment for age and femoral neck bone mineral density (adjusted OR: 1.62 to 2.40;  $p < 0.05$ ).

**Conclusions:** Despite similar bone mineral density values by dual x-ray absorptiometry, premenopausal women with a distal radial fracture have significantly poorer bone microarchitecture at the distal end of the radius and tibia compared with control subjects without a fracture. Early identification of women with poor bone health offers opportunities for interventions aimed at preventing further deterioration and reducing fracture risk.

**Level of Evidence:** Diagnostic Level I. See Instructions for Authors for a complete description of levels of evidence.

**Disclosure:** One or more of the authors received payments or services, either directly or indirectly (i.e., via his or her institution), from a third party in support of an aspect of this work. In addition, one or more of the authors, or his or her institution, has had a financial relationship, in the thirty-six months prior to submission of this work, with an entity in the biomedical arena that could be perceived to influence or have the potential to influence what is written in this work. No author has had any other relationships, or has engaged in any other activities, that could be perceived to influence or have the potential to influence what is written in this work. The complete **Disclosures of Potential Conflicts of Interest** submitted by authors are always provided with the online version of the article.

Osteoporosis and fragility fractures are major public health issues with considerable social and economic costs<sup>1-4</sup>. Measurement of bone mineral density by dual x-ray absorptiometry and risk assessment by the Fracture Risk Assessment Tool (FRAX) model are currently the gold standard for the diagnosis of osteoporosis, and low bone density is a widely accepted major risk factor for fragility fracture<sup>5-8</sup>. Yet, bone mineral density does not always accurately reflect fracture risk and up to 50% of those who sustain fragility fractures do not have osteoporosis by bone mineral density testing<sup>7-9</sup>. FRAX can also have a poor sensitivity for fracture prediction<sup>10-12</sup>. As such, recent efforts have focused on more sophisticated imaging technology to more accurately assess bone strength and fracture risk determinants.

In vivo assessment of bone morphology and microarchitecture is now possible using high-resolution peripheral quantitative computed tomography (HR-pQCT). Studies utilizing this technology have demonstrated worse trabecular and cortical bone microarchitecture in postmenopausal women and older men with a history of fragility fractures<sup>13-21</sup>. In some instances, differences in bone microarchitecture remained after fracture, even after adjusting for lower bone mineral density<sup>14,17,22</sup>. Although bone loss is most prominent after menopause, bone density and microarchitecture begin to decline before then<sup>23-25</sup>. However, it is unknown whether premenopausal women who sustain fractures have evidence of poor bone architecture.

We hypothesized that premenopausal women with fractures of the distal end of the radius would have similar bone mineral density but worse bone microarchitecture compared with control subjects with no fracture history. To address this hypothesis, we compared trabecular and cortical bone microarchitecture assessed by HR-pQCT at the distal end of the radius and distal end of the tibia in premenopausal women with a recent distal radial fracture and that in control subjects without a fracture. In addition, we determined whether differences in bone microarchitecture were significant after adjustment for bone mineral density at the hip or distal end of the radius.

## Methods

### Patient Identification

Following approval by our institutional review boards, premenopausal women under the age of forty-five years were recruited at Beth Israel Deaconess Medical Center (Boston, Massachusetts) and Brigham and Women's Hospital (Boston, Massachusetts) by their treating orthopaedic surgeon. Consecutive patients presenting with a distal radial fracture were screened for inclusion. All subjects gave written informed consent before participation. Subjects were eligible for inclusion in the fracture group if they had a documented history of a fracture of the distal end of the radius within three months of presentation. Fractures occurring from low-energy falls (from a standing height or less) as well as high-energy injuries (falls from greater than a standing height, motor vehicle accidents, or sporting injuries) were included. Control subjects presenting for treatment of other upper extremity conditions (tendinitis, ganglion cysts, overuse syndromes, etc.) and had no history of fractures in adulthood (after the age of eighteen years) were recruited. Potential patients were excluded if they were pregnant or had endocrinopathies (insulin-dependent diabetes mellitus or thyroid disease) or metabolic bone disease (osteomalacia, osteoporosis, Paget disease, or primary hyperparathyroidism). Exposure to glucocorticoids and immunosuppressive medications constituted exclusion criteria, as did treatment with hormone replacement therapy, bisphosphonates, para-

thyroid hormone, selective estrogen receptor modulators, or aromatase inhibitors. Women with eating disorders were also excluded from participation. Of 144 patients screened, 120 were eligible for enrollment and agreed to participate. Of those patients, eight refused participation and sixteen were lost to follow-up (nine fracture patients and seven controls were enrolled in clinic but never presented for their dual x-ray absorptiometry and HR-pQCT examinations).

### Demographic Information and Medical History

At the time of enrollment, information on any history of fractures, reproductive and menstrual history (including contraceptive pill usage), smoking, alcohol and caffeine intake, physical activity (inactive, moderately inactive, moderately active, or active), and use of calcium and vitamin D supplements was recorded using standardized questionnaires<sup>26</sup>. Weight was measured on a calibrated scale, and height was measured using a stadiometer. Data on hand dominance, mechanism of injury, and type of treatment were collected at the time of enrollment. Primary care providers were contacted for any missing information.

### Fracture Treatment and Classification

On presentation to the orthopaedic clinic, patients with a nondisplaced fracture were treated with short arm casting until union. Fractures with substantial comminution and those that underwent manipulation in the emergency department were followed with weekly radiographs. Patients in whom reduction was maintained were transitioned to a short arm cast until union. Patients with a displaced fracture were offered surgical treatment. Details on the timing and type of surgical treatment were collected. The initial anteroposterior and lateral radiographs were reviewed, and fractures were classified according to the AO fracture classification system<sup>27</sup> by a fellowship-trained orthopaedic hand surgeon.

### HR-pQCT of the Distal End of the Radius and Distal End of the Tibia

Trabecular and cortical bone density and microarchitecture at the distal ends of the radius and tibia were assessed using HR-pQCT (XtremeCT; Scanco Medical, Brüttisellen, Switzerland), as previously reported<sup>13</sup>. Scans were made in the noninjured extremity for fracture patients and in the nondominant extremity for control subjects. Scans were acquired at an isotropic voxel size of 82  $\mu\text{m}$ . During scan acquisition, the arm of the patient was immobilized in an anatomically formed carbon-fiber shell. An anteroposterior scout radiograph was used to define the measurement region with a reference line manually placed at the end plate of the radius and tibia (Figs. 1-A through 1-D). The first CT slice was acquired 9.5 mm and 22.5 mm proximal to the reference line for the distal ends of the radius and tibia, respectively. At each skeletal site, 110 CT slices were acquired, thus delivering a three-dimensional representation of approximately 9 mm in the axial direction. The effective dose of radiation was  $<5 \mu\text{Sv}$  per measurement.

Using semiautomated three-dimensional software, we assessed total, trabecular, and cortical bone densities as well as morphology, including total cross-sectional area, trabecular thickness, number, separation, and the standard deviation of trabecular separation, which reflects the heterogeneity of the trabecular network, and cortical thickness. Reproducibility, calculated from repeat scans on twenty-five young individuals, ranged from 0.2% to 1.7% for density values and from 0.7% to 8.6% for microarchitecture variables, consistent with prior reports<sup>13,23</sup>.

### Bone Mineral Density

Areal bone mineral density (expressed in grams per square centimeter) of the hip, spine, and forearm (distal one-third of the radius and ultradistal end of the radius) was measured by dual x-ray absorptiometry (QDR 4500; Hologic, Bedford, Massachusetts) in the array (fan beam) mode.

### Statistical Methods

The Student t test was used to compare age at diagnosis, age at menarche, and body mass index (BMI) between the forty patients with a fracture and the eighty control subjects without a fracture. Menstrual history, coffee and

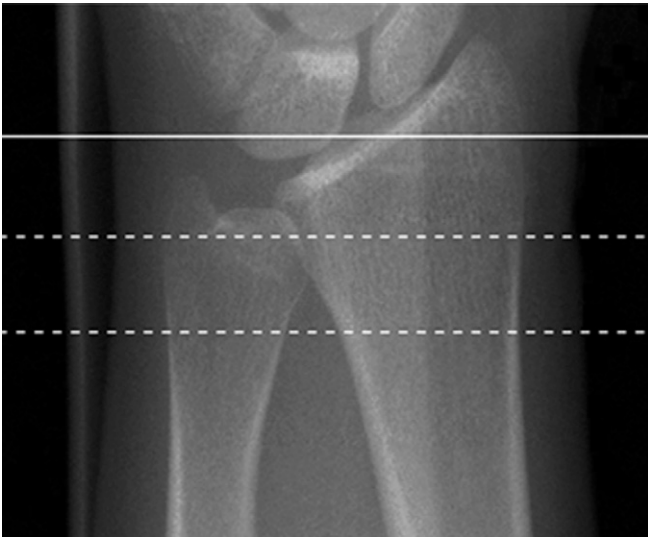


Fig. 1-A

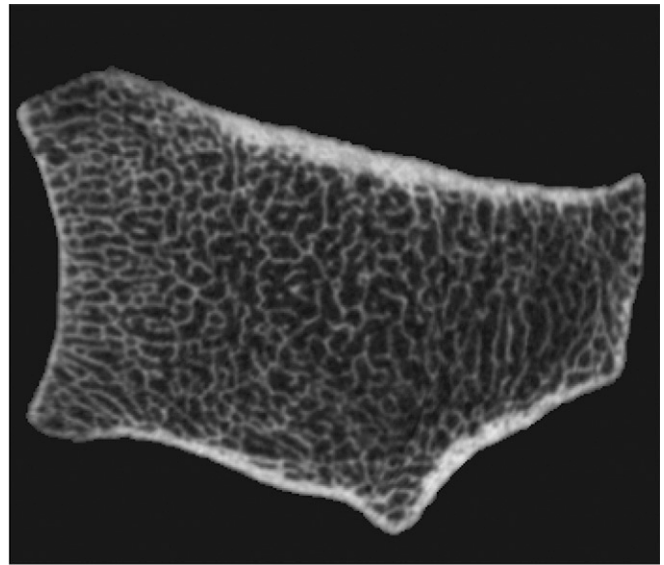


Fig. 1-B



Fig. 1-C

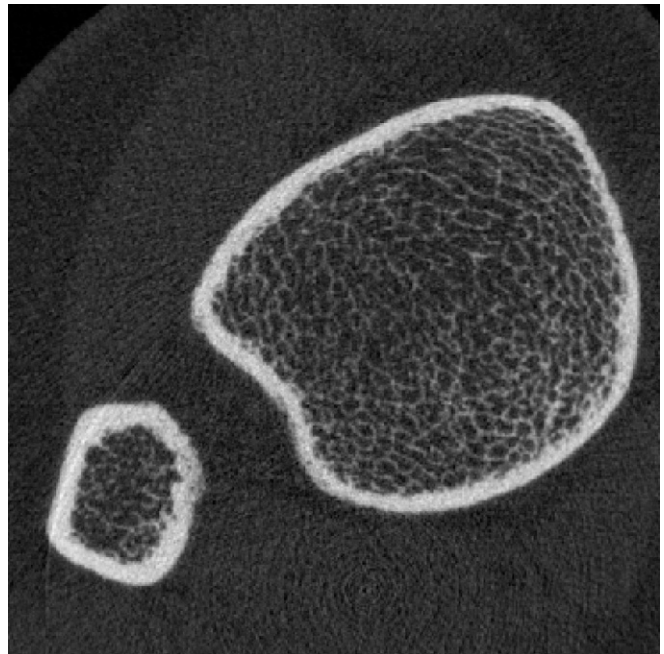


Fig. 1-D

**Figs. 1-A through 1-D** HR-pQCT imaging of the distal ends of the radius and tibia. **Fig. 1-A** Standard anteroposterior scout radiograph of the distal end of the radius, showing the placement of a reference line (solid line) and the volume of interest where CT slices are acquired (between dashed lines). **Fig. 1-B** Two-dimensional CT slice in the distal end of the radius, obtained with an XtremeCT scanner, showing the ability of the device to assess trabecular and cortical microarchitecture. **Fig. 1-C** Standard anteroposterior scout radiograph of the distal end of the tibia, showing the placement of a reference line (solid line) and the volume of interest where CT slices are acquired (between dashed lines). **Fig. 1-D** Two-dimensional CT slice obtained with the XtremeCT scanner in the distal end of the tibia, showing the ability of the device to assess trabecular and cortical microarchitecture.

alcohol consumption, as well as physical activity were compared between groups using the Mann-Whitney U test with medians and ranges reported for the groups. The Fisher exact test was used to compare categorical variables, except for race, which was compared with the chi-square test. Densities and bone architectural measurements for the distal end of the radius and distal end of the tibia, determined by dual x-ray absorptiometry and HR-pQCT, were compared using the Student t test for univariate analysis. Unadjusted analysis and analysis after adjustments for age, bone mineral density of the

femoral neck, and bone mineral density of the ultradistal end of the radius were performed using logistic regression to determine the odds of fracture expressed per one-unit change in standard deviation, with 95% confidence intervals (CI). A two-tailed p value of <0.05 was considered significant. All statistical analyses were conducted using SAS software (version 9.2; SAS Institute, Cary, North Carolina).

Sample size estimates were derived from prior data comparing bone microarchitecture by HR-pQCT in postmenopausal fracture patients. Our

**TABLE 1** Comparison of Bone Mineral Density at the Hip, Spine, and Forearm in Subjects with and without a Fracture of the Distal End of the Radius

Variable*	Fracture Group† (N = 40)	Control Group† (N = 80)	P Value
Spine BMD ( $g/cm^2$ )	1.022 ± 0.123	1.126 ± 0.816	0.425
Femoral neck BMD ( $g/cm^2$ )	0.837 ± 0.115	0.875 ± 0.134	0.134
Total hip BMD ( $g/cm^2$ )	0.939 ± 0.101	0.984 ± 0.132	0.061
BMD of ultradistal end of radius ( $g/cm^2$ )	0.436 ± 0.079	0.462 ± 0.067	0.063
BMD of distal third of radius ( $g/cm^2$ )	0.707 ± 0.067	0.720 ± 0.055	0.259

\*BMD = bone mineral density. †The values are given as the mean and the standard deviation.

power analysis indicated that sample sizes of forty patients with a fracture and eighty age-matched control subjects provided 80% power to detect a mean difference of 10% in each density and structural parameter, assuming a standard deviation of 20% (moderate effect size = 0.50) using the Student t test with a two-tailed alpha level of 0.05 (version 7.0, nQuery Advisor; Statistical Solutions, Saugus, Massachusetts).

#### Source of Funding

This work was supported by a Clinical Research Grant from the Ruth Jackson Orthopaedic Society and Zimmer, Inc., as well as Sanofi LLC. Purchase of the HR-pQCT machine was made possible through a shared equipment grant from the National Center for Research Resources (NIH/NCRR 1 S10 RR023405).

## Results

### Patient Characteristics

Forty fracture patients and eighty control subjects were enrolled. The fracture and control groups were similar in their demographic characteristics and medical conditions (see Appendix). Subjects did not differ with respect to age, race, or BMI. The average time (and standard deviation) between fracture and scan acquisition was 49 ± 50 days (range, six to 191 days).

Among fracture patients, twenty-three injuries were sustained from a fall from a standing height, fifteen from high-energy

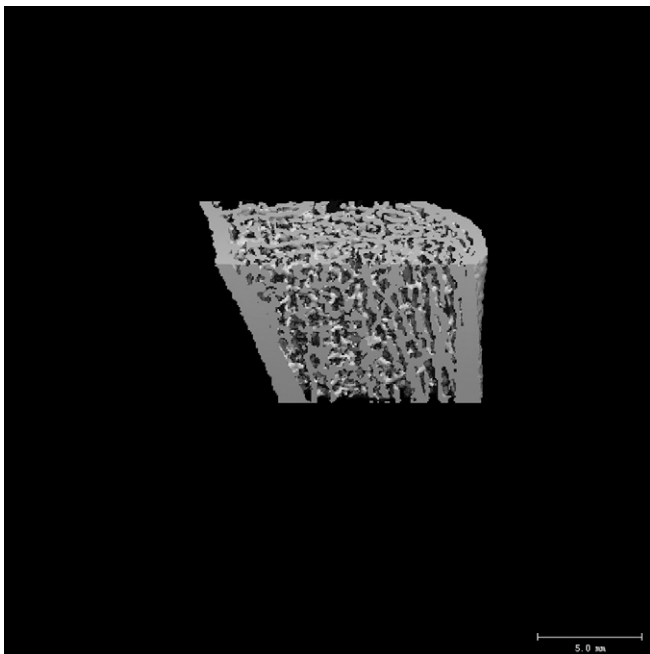


Fig. 2-A

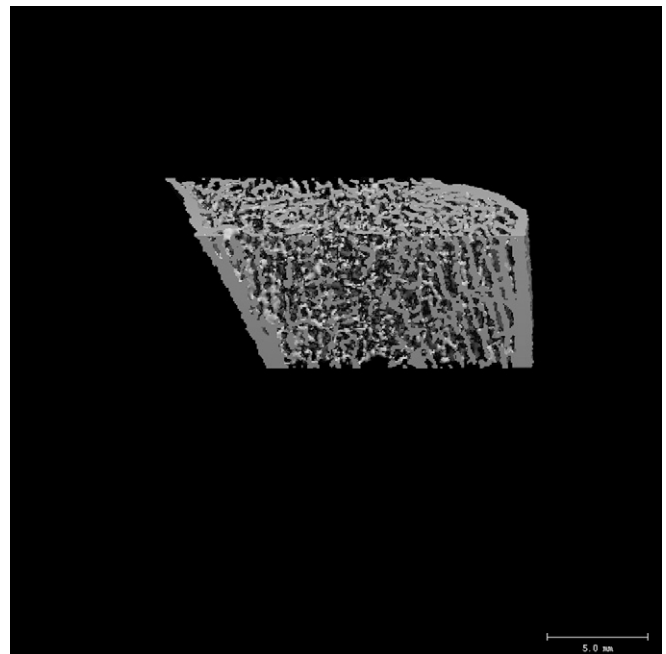


Fig. 2-B

**Fig. 2-A and 2-B** Representative three-dimensional reconstructions of images of the distal end of the radius obtained with HR-pQCT. **Fig. 2-A** The distal end of the radius in an age-matched control subject (bone mineral density of the ultradistal end of the radius = 0.446  $g/cm^2$ , trabecular density = 199  $mg/cm^3$ , and cortical thickness = 0.87 mm). **Fig. 2-B** The distal end of the radius in a fracture patient (bone mineral density of the ultradistal end of the radius = 0.446  $g/cm^2$ , trabecular density = 145  $mg/cm^3$ , and cortical thickness = 0.71 mm) with similar areal bone mineral density values at the ultradistal end of the radius. Compared with the control subject, the fracture patient had lower trabecular density, number, and thickness and higher trabecular separation.

TABLE II Comparison of HR-pQCT-Derived Volumetric Densities and Bone Microarchitecture Measures in Fracture and Control Groups

Variable	Distal End of Radius			Distal End of Tibia		
	Fracture* (N = 40)	Controls* (N = 80)	P Value	Fracture* (N = 40)	Controls* (N = 80)	P Value
Total density (mg HA/cm <sup>3</sup> )	304 ± 57	327 ± 51	0.026	293 ± 47	328 ± 52	0.001
Trabecular density (mg HA/cm <sup>3</sup> )	146 ± 32	172 ± 33	<0.001	156 ± 32	182 ± 37	<0.001
Cortical bone density (mg HA/cm <sup>3</sup> )	866 ± 50	866 ± 49	0.983	894 ± 39	902 ± 33	0.22
Total area (mm <sup>2</sup> )	263 ± 42	257 ± 43	0.48	668 ± 122	651 ± 110	0.44
Trabecular area (mm <sup>2</sup> )	212 ± 42	205 ± 43	0.46	551 ± 123	525 ± 112	0.24
Cortical area (mm <sup>2</sup> )	51 ± 10	52 ± 10	0.88	117 ± 16	126 ± 20	0.014
Trabecular thickness (mm)	0.06 ± 0.01	0.07 ± 0.01	0.002	0.07 ± 0.01	0.08 ± 0.01	0.005
Trabecular number (mm <sup>-1</sup> )	1.89 ± 0.36	2.02 ± 0.23	0.032	1.82 ± 0.34	1.93 ± 0.31	0.13
Trabecular separation (mm)	0.49 ± 0.15	0.43 ± 0.06	0.014	0.50 ± 0.13	0.46 ± 0.09	0.037
Stand. dev. of trabecular separation (mm)	0.22 ± 0.12	0.17 ± 0.03	0.032	0.24 ± 0.14	0.21 ± 0.06	0.068
Cortical thickness (mm)	0.76 ± 0.15	0.77 ± 0.15	0.57	1.17 ± 0.19	1.28 ± 0.23	0.014

\*The values are given as the mean and the standard deviation.

sports, and two from motor vehicle accidents. Twenty-two patients fractured the dominant extremity. According to the AO classification, twelve fractures were type A (six were type A1; five, type A2; and one, type A3), two were type B (one was type B1; one, type B2; and none were type B3), and twenty-six were type C (eight were type C1; eleven, type C2; and seven, type C3). Twenty-five fractures were treated with casting, and fifteen underwent operative fixation with a volar plate. All healed without complications.

#### Bone Mineral Density by Dual X-Ray Absorptiometry

Bone mineral density was similar between the fracture and control groups at the femoral neck, spine, and distal end of the radius (Table I). Although the difference was not significant, bone mineral density tended to be lower in the fracture group at the hip and ultradistal end of the radius ( $p = 0.06$ ).

#### Microarchitecture by HR-pQCT

Cortical and trabecular microarchitecture differed between groups both at the distal end of the radius and the distal end of the tibia (Table II, Figs. 2-A, 2-B, and 3). At the distal end of the radius, the fracture group had lower total density ( $-7\%$ ;  $p = 0.026$ ), trabecular density ( $-15\%$ ;  $p < 0.001$ ), trabecular thickness ( $-14\%$ ;  $p = 0.002$ ), and trabecular number ( $-6\%$ ;  $p = 0.03$ ) than the control subjects without a fracture. Trabecular separation was greater among the fracture group ( $+14\%$ ;  $p = 0.014$ ). Cortical density and morphology at the distal end of the radius did not differ between groups.

At the distal end of the tibia, the fracture group had lower values than the control group with respect to total density ( $-11\%$ ;  $p = 0.001$ ), trabecular density ( $-14\%$ ;  $p < 0.001$ ), and trabecular thickness ( $-13\%$ ;  $p = 0.005$ ). Trabecular separation was greater among the fracture group ( $+9\%$ ;  $p = 0.037$ ). In

addition, the fracture group had lower cortical area ( $-7\%$ ;  $p = 0.014$ ) and cortical thickness ( $-9\%$ ;  $p = 0.014$ ). These results are summarized in Figure 3.

The odds ratios for fracture, before and after adjustment for age and bone mineral density, are shown in Table III. Many

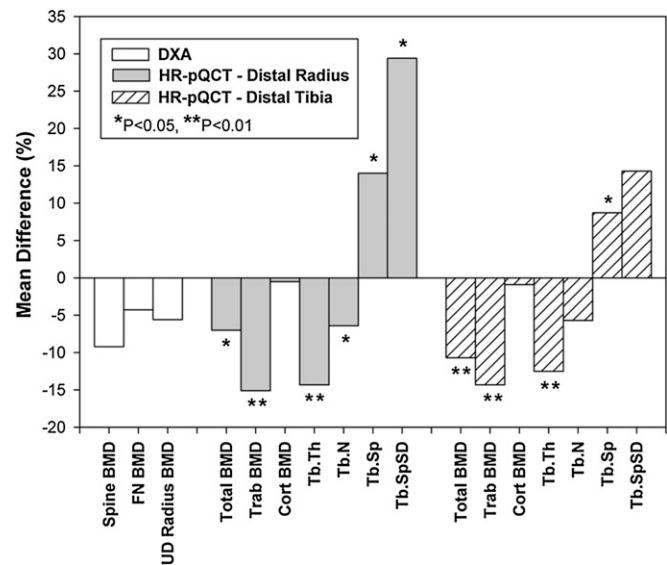


Fig. 3

The mean differences in bone mineral density (BMD) and bone microarchitecture between the fracture and control groups. FN = femoral neck, UD = ultradistal, Trab = trabecular, cort = cortical, Tb.Th = trabecular thickness, Tb.N = trabecular number, Tb.Sp = trabecular separation, Tb.SpSD = standard deviation of trabecular separation, HR-pQCT = high-resolution peripheral quantitative computed tomography, and DXA = dual x-ray absorptiometry.



**TABLE III Relative Risk for Wrist Fracture Expressed as Odds Ratio per Standard Deviation Difference, Including Unadjusted Analyses and Analyses Adjusted for Age and Bone Mineral Density of Hip or Ultradistal End of Radius\***

Variable	Unadjusted		Adjusted for Age and Femoral Neck BMD		Adjusted for Age and Ultradistal Radial BMD	
	OR (95% CI)	P Value	OR (95% CI)	P Value	OR (95% CI)	P Value
<b>Dual x-ray absorptiometry</b>						
Spine BMD	1.56 (0.38–6.32)	0.54	1.36 (0.48-3.84)	0.56	1.40 (0.43-4.61)	0.58
Femoral neck BMD	1.36 (0.91-2.03)	0.14	–	–	1.14 (0.71-1.83)	0.60
Total hip BMD	1.48 (0.98-2.24)	0.06	1.79 (0.70-4.58)	0.22	1.28 (0.78-2.11)	0.32
BMD of ultradistal end of radius	1.52 (0.97-2.39)	0.07	1.40 (0.83-2.36)	0.21	–	–
BMD of distal third of radius	1.24 (0.85-1.82)	0.26	–	–	–	–
<b>HR-pQCT of radius</b>						
Total density	1.58 (1.05-2.39)	0.029	1.52 (0.98-2.36)	0.07	1.53 (0.89-2.64)	0.13
Trabecular density	2.42 (1.49-3.92)	<0.001	2.58 (1.48-4.51)	0.001	2.98 (1.57-5.67)	0.001
Cortical bone density	1.00 (0.69-1.47)	0.98	1.00 (0.68-1.49)	0.98	0.88 (0.56-1.37)	0.56
Total area	0.87 (0.60-1.27)	0.48	0.83 (0.56-1.22)	0.34	0.86 (0.58-1.26)	0.43
Trabecular area	0.87 (0.59-1.27)	0.46	0.84 (0.57-1.24)	0.38	0.89 (0.60-1.31)	0.55
Cortical area	1.03 (0.70-1.51)	0.88	0.94 (0.62-1.43)	0.77	0.75 (0.44-1.26)	0.27
Trabecular thickness	2.05 (1.27-3.32)	0.003	1.94 (1.18-3.21)	0.010	2.01 (1.13-3.58)	0.018
Trabecular number	1.65 (1.10-2.48)	0.017	1.55 (0.99-2.42)	0.06	1.50 (0.95-2.35)	0.08
Trabecular separation	2.16 (1.26-3.73)	0.006	2.10 (1.16-3.80)	0.015	2.02 (1.10-3.71)	0.023
Stand. dev. of trabecular separation†	2.90 (1.38-6.08)	0.005	2.71 (1.23-5.98)	0.013	2.61 (1.16-5.90)	0.021
Cortical thickness	1.12 (0.76-1.64)	0.57	1.05 (0.70-1.57)	0.82	0.87 (0.53-1.45)	0.60
<b>HR-pQCT of tibia</b>						
Total density	2.14 (1.35-3.41)	0.001	2.06 (1.24-3.44)	0.006	2.12 (1.21-3.72)	0.009
Trabecular density	2.19 (1.37-3.47)	0.001	2.40 (1.31-4.38)	0.005	2.14 (1.23-3.71)	0.007
Cortical bone density	1.27 (0.86-1.88)	0.22	1.29 (0.86-1.93)	0.23	1.16 (0.74-1.81)	0.51
Total area	0.86 (0.58-1.26)	0.44	0.79 (0.52-1.19)	0.25	0.91 (0.61-1.36)	0.65
Trabecular area	0.79 (0.54-1.17)	0.24	0.75 (0.50-1.13)	0.16	0.87 (0.58-1.30)	0.50
Cortical area	1.69 (1.10-2.59)	0.017	1.68 (1.00-2.82)	0.048	1.59 (0.94-2.71)	0.10
Trabecular thickness	1.88 (1.19-2.96)	0.007	1.81 (1.11-2.95)	0.018	1.73 (1.05-2.85)	0.031
Trabecular number	1.36 (0.91-2.03)	0.13	1.14 (0.70-1.85)	0.60	1.16 (0.76-1.79)	0.49
Trabecular separation	1.51 (1.00-2.27)	0.049	1.32 (0.82-2.15)	0.26	1.30 (0.84-2.02)	0.24
Stand. dev. of trabecular separation†	1.49 (0.90-2.46)	0.12	1.26 (0.76-2.08)	0.37	1.25 (0.78-2.01)	0.35
Cortical thickness	1.69 (1.10-2.59)	0.016	1.62 (1.02-2.57)	0.041	1.57 (0.93-2.66)	0.09

\*BMD = bone mineral density, OR = odds ratio, and CI = confidence interval. †Odds ratio per standard deviation decrease (all variables, except trabecular separation and standard deviation of trabecular separation, which are calculated per standard deviation increase).

of the differences in bone microarchitecture between the fracture and control groups remained significant after adjusting for age and hip bone mineral density or for age and ultradistal radial bone mineral density. In unadjusted analyses, odds ratios for a change of one standard deviation in bone microarchitecture at the radius ranged from 1.58 (95% CI: 1.05 to 2.39) for total density to 2.90 (95% CI: 1.38 to 6.08) for the distribution of trabecular separation. After adjustment for age and hip bone mineral density or age and ultradistal radial bone mineral density,

the radial trabecular density, thickness, separation, and distribution of trabecular separation remained associated with fracture (adjusted odds ratios, 1.94 to 2.98).

At the tibia, unadjusted odds ratios ranged from 1.51 (95% CI: 1.00 to 2.27) for trabecular separation to 2.19 (95% CI: 1.37 to 3.47) for trabecular density. After adjustment for age and femoral neck bone mineral density, the total density, trabecular density, trabecular thickness, cortical area, and cortical thickness remained significantly associated with fracture

(adjusted odds ratios, 1.62 to 2.40). After adjusting for age and ultradistal radial bone mineral density, the total density, trabecular density, and trabecular thickness remained associated with fracture, whereas cortical area ( $p = 0.10$ ) and thickness ( $p = 0.09$ ) were no longer significantly associated with fracture.

Trabecular and cortical densities were moderately correlated with total density ( $r = 0.68$  and  $r = 0.73$ , respectively). At the radius, trabecular number ( $r = 0.72$ ) and thickness ( $r = 0.73$ ) positively correlated with trabecular density, whereas separation ( $r = -0.73$ ) and distribution of trabecular separation ( $r = -0.59$ ) inversely correlated with trabecular density. For the tibia, trabecular density had a moderate positive correlation with trabecular number ( $r = 0.61$ ) and thickness ( $r = 0.64$ ) as well as with cortical area ( $r = 0.50$ ) and cortical thickness ( $r = 0.45$ ). Cortical density was not significantly correlated to trabecular density ( $r = -0.05$ ).

### Discussion

Pre-menopausal women with a recent distal radial fracture have significantly poorer volumetric bone density and microarchitecture at the distal end of the radius and tibia compared with control subjects without a fracture. Specifically, women with fractures had lower total and trabecular bone density, as well as decreased trabecular number and thickness at both the distal end of the radius and distal end of the tibia. The fracture group also had lower cortical density and thickness at the distal end of the tibia. These differences remained after adjusting for age and bone mineral density at the hip and ultradistal end of the radius.

Studies have shown that bone loss associated with osteoporosis is accompanied by deterioration in bone architecture, increasing the susceptibility to fracture. Recent advances in high-resolution imaging allowing quantification of trabecular and cortical bone microarchitecture have advanced our understanding of changes in bone mass and geometry<sup>23,28</sup>. Furthermore, deteriorated cortical and trabecular microarchitecture, as measured by HR-pQCT<sup>13,29</sup> and high-resolution magnetic resonance imaging<sup>30</sup>, have been associated with fragility fractures in postmenopausal women, independently of bone mineral density. Our study revealed that the fracture and control groups were similar with respect to bone mineral density and that differences in microarchitecture were independent of bone mineral density by dual x-ray absorptiometry. This suggests that HR-pQCT detects differences in osseous architecture that are not measured by dual x-ray absorptiometry scans alone.

The relationship between bone microarchitecture and fractures in postmenopausal women and older men has been studied previously<sup>14,19,21</sup>. The results have indicated that postmenopausal women with a history of fragility fractures have lower total and trabecular bone density, trabecular thickness, and trabecular number after adjusting for hip bone mineral density. Older men with a history of fragility fractures also have deteriorated trabecular and cortical architecture compared with age-matched control subjects without a fracture<sup>18</sup>. To date, the use of these imaging modalities in premenopausal patients has been limited and, despite the potential of identifying the early stages of skeletal fragility, we are not aware of any studies ex-

amining bone density and microarchitecture in otherwise normal premenopausal women with fractures.

Some studies have described lower bone mineral density in adolescents with forearm fractures, as well as higher rates of refracture, than in control subjects<sup>31,32</sup>. Other studies, however, have noted that fractures in childhood do not predict fractures in adulthood<sup>33</sup>. A number of studies have demonstrated that bone loss begins in early adulthood once peak bone mass is attained<sup>34</sup> and, accordingly, fractures in early adulthood may be important risk factors for subsequent fragility fractures. Identification of patients at risk for osteoporosis before menopause would provide a unique opportunity to initiate early treatment and prevention efforts to decrease future fractures.

Previous work has shown that premenopausal women with idiopathic osteoporosis have worse trabecular architecture at the radius and tibia and thinner cortices at the distal end of the tibia than normal age-matched controls<sup>35</sup>. The women in our study did not have low bone mineral density, and yet they had a similar pattern of poor trabecular architecture and thinner cortices at the distal end of the tibia. Our fracture group included low and high-energy distal radial fractures, suggesting that low bone mineral density and deteriorated microarchitecture may play a role not only in fragility fractures but also in all fracture types. A similar association between low bone mineral density and traumatic fracture risk in older men and women has been previously reported<sup>36</sup>.

Potential reasons for low bone mineral density in our patient population include genetic factors<sup>37,38</sup>, menstrual function<sup>39-41</sup>, oral contraceptive use<sup>42</sup>, poor dietary intake<sup>43,44</sup>, and lower physical activity<sup>45-47</sup>. Of these, late menarche and lower physical activity<sup>39,45,48,49</sup> lead to a deterioration of bone microarchitecture as measured by HR-pQCT. We obtained detailed information from our subjects and did not detect any significant differences between the fracture and control groups. More subtle variations, however, may have remained undetected, and genetic factors were not explored.

Study limitations include a predominantly white patient population representative of the New England region as well as a cross-sectional design, which does not allow future fracture prediction. There was some variability in the timing of obtaining dual x-ray absorptiometry and HR-pQCT scans in the fracture group, which may have influenced the results. Although it is possible that the changes in microarchitecture occurred after fracture, we believe this to be unlikely since the arm without a fracture was measured and it is unlikely to have undergone any changes due to disuse. Furthermore, we were unable to explore whether poor bone microarchitecture was related to low bone formation and/or high resorption. Although this could be examined using serum markers of bone turnover, these are known to increase after a fracture, remain elevated for up to a year, and may not have been helpful in our cohort<sup>50</sup>. We did explore clinical factors that may have been related to poorer bone microarchitecture in the patients with a fracture, but we found no differences between groups with respect to common risk factors for low bone mineral density and fracture.


The strength of the study lies in its focus on distal radial fracture. Although central fractures are associated with greater morbidity and may have shown greater differences in bone microarchitecture parameters, we chose to focus on distal radial fractures because these are among the most common injuries in young adults<sup>51,52</sup> and the second most common fragility fracture in postmenopausal women<sup>53,54</sup>. Also, the pediatric literature has demonstrated that wrist and forearm fractures in children and young adolescents are associated with a decrease in bone mineral density<sup>31,32</sup>. Third, distal radial fractures in adults typically occur at an earlier age than fractures of the hip or spine<sup>23,55-57</sup>, offering a unique opportunity to initiate treatment for underlying abnormalities in bone structure and metabolism. These fractures are an important cohort to study in the setting of osteoporosis and fracture risk. In addition, our study is unique in that it compares osseous microarchitecture in premenopausal women with and without fractures. We were able to obtain all measurements relatively soon after fracture and limited the number of potential confounders by applying strict inclusion and exclusion criteria. Finally, this is the first study we are aware of to demonstrate differences in trabecular microarchitecture after adjusting for bone mineral density at the ultradistal end of the radius.

Current case management strategies are focused on identifying postmenopausal women with clinical factors and low bone mineral density who are at increased risk for fracture, and targeting them for pharmacologic intervention<sup>58-60</sup>. While this may reduce fracture risk, this approach may be limited in that bone mineral density is already substantially decreased at the time of intervention and compliance with osteoporosis medications is generally poor<sup>61-64</sup>. Moreover, the majority of currently approved therapies are designed to inhibit further bone loss, rather than to promote bone gain to prior levels. Recent population-based studies have found that women experienced a significant decline in trabecular bone mass and architecture before menopause<sup>23,28</sup>. Thus, an alternative approach to treating those at high risk for fractures would identify premenopausal women with early signs of skeletal fragility and initiate lifestyle and/or pharmacologic interventions to prevent further skeletal deterioration and reduce future fracture burden.

In conclusion, premenopausal women with a recent distal radial fracture have similar bone mineral density but worse microarchitecture compared with control subjects with no history

of fracture. Although limited by the cross-sectional study design, our results suggest that poor bone microarchitecture at a younger age may be an important risk factor for fractures. Future work identifying patients at risk of osteoporosis before menopause may extend on our findings and provide opportunities to initiate early treatment and prevention efforts.

### Appendix

 A table showing the demographic characteristics of the fracture and control groups is available with the online version of this article as a data supplement at [jbjs.org](http://jbjs.org). ■

Tamara D. Rozental, MD  
Laura N. Deschamps, BA  
Charles S. Day, MD  
Department of Orthopaedic Surgery,  
Beth Israel Deaconess Medical Center,  
330 Brookline Avenue, Stoneman 10,  
Boston, MA 02215

Alexander Taylor, BA  
Department of Medicine, Endocrine Division,  
Massachusetts General Hospital,  
50 Blossom Street, Thier 1051,  
Boston, MA 02114

Brandon Earp, MD  
Department of Orthopaedic Surgery,  
Brigham and Women's Hospital,  
75 Francis Street,  
A Building, Boston, MA 02215

David Zurakowski, PhD  
Departments of Anesthesia and Surgery,  
Boston Children's Hospital,  
300 Longwood Avenue,  
Boston MA 02115

Mary L. Boussein, PhD  
Department of Orthopaedic Surgery,  
Beth Israel Deaconess Medical Center,  
Orthopedic Biomechanics Laboratory,  
RN 115, 330 Brookline Ave,  
Boston, MA 02215

### References

1. Looker AC, Orwoll ES, Johnston CC Jr, Lindsay RL, Wahner HW, Dunn WL, Calvo MS, Harris TB, Heyse SP. Prevalence of low femoral bone density in older U.S. adults from NHANES III. *J Bone Miner Res.* 1997 Nov;12(11):1761-8.
2. Court-Brown CM, Caesar B. Epidemiology of adult fractures: A review. *Injury.* 2006 Aug;37(8):691-7.
3. Burge R, Dawson-Hughes B, Solomon DH, Wong JB, King A, Tosteson A. Incidence and economic burden of osteoporosis-related fractures in the United States, 2005-2025. *J Bone Miner Res.* 2007 Mar;22(3):465-75.
4. Cummings SR, Melton LJ. Epidemiology and outcomes of osteoporotic fractures. *Lancet.* 2002 May 18;359(9319):1761-7.
5. Kanis JA, Johnell O, Oden A, Dawson A, De Laet C, Jonsson B. Ten year probabilities of osteoporotic fractures according to BMD and diagnostic thresholds. *Osteoporos Int.* 2001 Dec;12(12):989-95.
6. Kanis JA, Johnell O, De Laet C, Jonsson B, Oden A, Ogelsby AK. International variations in hip fracture probabilities: implications for risk assessment. *J Bone Miner Res.* 2002 Jul;17(7):1237-44.
7. Stone KL, Seeley DG, Lui LY, Cauley JA, Ensrud K, Browner WS, Nevitt MC, Cummings SR; Osteoporotic Fractures Research Group. BMD at multiple sites and risk of fracture of multiple types: long-term results from the Study of Osteoporotic Fractures. *J Bone Miner Res.* 2003 Nov;18(11):1947-54.
8. Wainwright SA, Marshall LM, Ensrud KE, Cauley JA, Black DM, Hillier TA, Hochberg MC, Vogt MT, Orwoll ES; Study of Osteoporotic Fractures Research Group. Hip fracture in women without osteoporosis. *J Clin Endocrinol Metab.* 2005 May;90(5):2787-93.
9. Schuit SC, van der Klift M, Weel AE, de Laet CE, Burger H, Seeman E, Hofman A, Uitterlinden AG, van Leeuwen JP, Pols HA. Fracture incidence and association with



- bone mineral density in elderly men and women: the Rotterdam Study. *Bone*. 2004 Jan;34(1):195-202.
10. Leslie WD, Lix LM, Johansson H, Oden A, McCloskey E, Kanis JA; Manitoba Bone Density Program. Independent clinical validation of a Canadian FRAX tool: fracture prediction and model calibration. *J Bone Miner Res*. 2010 Nov;25(11):2350-8.
  11. Trémollières FA, Pouillès JM, Drewniak N, Laparra J, Ribot CA, Dargent-Molina P. Fracture risk prediction using BMD and clinical risk factors in early postmenopausal women: sensitivity of the WHO FRAX tool. *J Bone Miner Res*. 2010 May;25(5):1002-9.
  12. Pressman AR, Lo JC, Chandra M, Ettinger B. Methods for assessing fracture risk prediction models: experience with FRAX in a large integrated health care delivery system. *J Clin Densitom*. 2011 Oct-Dec;14(4):407-15.
  13. Boutroy S, Boussein ML, Munoz F, Delmas PD. In vivo assessment of trabecular bone microarchitecture by high-resolution peripheral quantitative computed tomography. *J Clin Endocrinol Metab*. 2005 Dec;90(12):6508-15.
  14. Sornay-Rendu E, Boutroy S, Munoz F, Delmas PD. Alterations of cortical and trabecular architecture are associated with fractures in postmenopausal women, partially independent of decreased BMD measured by DXA: the OFELY study. *J Bone Miner Res*. 2007 Mar;22(3):425-33.
  15. Vico L, Zouch M, Amirouche A, Frère D, Laroche N, Koller B, Laib A, Thomas T, Alexandre C. High-resolution pQCT analysis at the distal radius and tibia discriminates patients with recent wrist and femoral neck fractures. *J Bone Miner Res*. 2008 Nov;23(11):1741-50.
  16. Vilayphiou N, Boutroy S, Sornay-Rendu E, Van Rietbergen B, Munoz F, Delmas PD, Chapurlat R. Finite element analysis performed on radius and tibia HR-pQCT images and fragility fractures at all sites in postmenopausal women. *Bone*. 2010 Apr;46(4):1030-7.
  17. Szulc P, Boutroy S, Vilayphiou N, Chaitou A, Delmas PD, Chapurlat R. Cross-sectional analysis of the association between fragility fractures and bone microarchitecture in older men: the STRAMBO study. *J Bone Miner Res*. 2011 Jun;26(6):1358-67.
  18. Vilayphiou N, Boutroy S, Szulc P, van Rietbergen B, Munoz F, Delmas PD, Chapurlat R. Finite element analysis performed on radius and tibia HR-pQCT images and fragility fractures at all sites in men. *J Bone Miner Res*. 2011 May;26(5):965-73.
  19. Liu XS, Stein EM, Zhou B, Zhang CA, Nickolas TL, Cohen A, Thomas V, McMahon DJ, Cosman F, Nieves J, Shane E, Guo XE. Individual trabecula segmentation (ITS)-based morphological analyses and microfinite element analysis of HR-pQCT images discriminate postmenopausal fragility fractures independent of DXA measurements. *J Bone Miner Res*. 2012 Feb;27(2):263-72.
  20. Melton LJ 3rd. Application of technology to push epidemiology forward. *Osteoporos Int*. 2009 May;20(Suppl 3):S235-6.
  21. Stein EM, Liu XS, Nickolas TL, Cohen A, Thomas V, McMahon DJ, Zhang C, Yin PT, Cosman F, Nieves J, Guo XE, Shane E. Abnormal microarchitecture and reduced stiffness at the radius and tibia in postmenopausal women with fractures. *J Bone Miner Res*. 2010 Dec;25(12):2572-81.
  22. Liu XS, Cohen A, Shane E, Yin PT, Stein EM, Rogers H, Kokolus SL, McMahon DJ, Lappe JM, Recker RR, Lang T, Guo XE. Bone density, geometry, microstructure, and stiffness: Relationships between peripheral and central skeletal sites assessed by DXA, HR-pQCT, and cQCT in premenopausal women. *J Bone Miner Res*. 2010 Oct;25(10):2229-38.
  23. Khosla S, Riggs BL, Atkinson EJ, Oberg AL, McDaniel LJ, Holets M, Peterson JM, Melton LJ 3rd. Effects of sex and age on bone microstructure at the ultradistal radius: a population-based noninvasive in vivo assessment. *J Bone Miner Res*. 2006 Jan;21(1):124-31.
  24. Riggs BL, Melton LJ 3rd, Robb RA, Camp JJ, Atkinson EJ, Peterson JM, Rouleau PA, McCollough CH, Boussein ML, Khosla S. Population-based study of age and sex differences in bone volumetric density, size, geometry, and structure at different skeletal sites. *J Bone Miner Res*. 2004 Dec;19(12):1945-54.
  25. Macdonald HM, Nishiyama KK, Kang J, Hanley DA, Boyd SK. Age-related patterns of trabecular and cortical bone loss differ between sexes and skeletal sites: a population-based HR-pQCT study. *J Bone Miner Res*. 2011 Jan;26(1):50-62.
  26. Wareham NJ, Jakes RW, Rennie KL, Schuit J, Mitchell J, Hennings S, Day NE. Validity and repeatability of a simple index derived from the short physical activity questionnaire used in the European Prospective Investigation into Cancer and Nutrition (EPIC) study. *Public Health Nutr*. 2003 Jun;6(4):407-13.
  27. Müller M, Nazarian S, Koch P, Schatzker J. The comprehensive classification of fractures of long bones. 1st ed. Berlin, Heidelberg, New York: Springer-Verlag; 1990.
  28. Riggs BL, Melton LJ, Robb RA, Camp JJ, Atkinson EJ, McDaniel L, Amin S, Rouleau PA, Khosla S. A population-based assessment of rates of bone loss at multiple skeletal sites: evidence for substantial trabecular bone loss in young adult women and men. *J Bone Miner Res*. 2008 Feb;23(2):205-14.
  29. Boutroy S, Van Rietbergen B, Sornay-Rendu E, Munoz F, Boussein ML, Delmas PD. Finite element analysis based on in vivo HR-pQCT images of the distal radius is associated with wrist fracture in postmenopausal women. *J Bone Miner Res*. 2008 Mar;23(3):392-9.
  30. Wehrli FW. Structural and functional assessment of trabecular and cortical bone by micro magnetic resonance imaging. *J Magn Reson Imaging*. 2007 Feb;25(2):390-409.
  31. Goulding A, Cannan R, Williams SM, Gold EJ, Taylor RW, Lewis-Barned NJ. Bone mineral density in girls with forearm fractures. *J Bone Miner Res*. 1998 Jan;13(1):143-8.
  32. Goulding A, Grant AM, Williams SM. Bone and body composition of children and adolescents with repeated forearm fractures. *J Bone Miner Res*. 2005 Dec;20(12):2090-6.
  33. Pye SR, Tobias J, Silman AJ, Reeve J, O'Neill TW; EPOS Study Group. Childhood fractures do not predict future fractures: results from the European Prospective Osteoporosis Study. *J Bone Miner Res*. 2009 Jul;24(7):1314-8.
  34. Matkovic V, Jelic T, Wardlaw GM, Ilich JZ, Goel PK, Wright JK, Andon MB, Smith KT, Heaney RP. Timing of peak bone mass in Caucasian females and its implication for the prevention of osteoporosis. Inference from a cross-sectional model. *J Clin Invest*. 1994 Feb;93(2):799-808.
  35. Cohen A, Liu XS, Stein EM, McMahon DJ, Rogers HF, Lemaster J, Recker RR, Lappe JM, Guo XE, Shane E. Bone microarchitecture and stiffness in premenopausal women with idiopathic osteoporosis. *J Clin Endocrinol Metab*. 2009 Nov;94(11):4351-60.
  36. Mackey DC, Lui LY, Cawthon PM, Bauer DC, Nevitt MC, Cauley JA, Hillier TA, Lewis CE, Barrett-Connor E, Cummings SR; Study of Osteoporotic Fractures (SOF) and Osteoporotic Fractures in Men Study (MrOS) Research Groups. High-trauma fractures and low bone mineral density in older women and men. *JAMA*. 2007 Nov 28;298(20):2381-8.
  37. Sigurdsson G, Halldorsson BV, Styrkarsdottir U, Kristjansson K, Stefansson K. Impact of genetics on low bone mass in adults. *J Bone Miner Res*. 2008 Oct;23(10):1584-90.
  38. Fox KM, Cummings SR, Powell-Threets K, Stone K; Study of Osteoporotic Fractures Research Group. Family history and risk of osteoporotic fracture. *Osteoporos Int*. 1998;8(6):557-62.
  39. Chevalley T, Bonjour JP, Ferrari S, Rizzoli R. Deleterious effect of late menarche on distal tibia microstructure in healthy 20-year-old and premenopausal middle-aged women. *J Bone Miner Res*. 2009 Jan;24(1):144-52.
  40. Armamento-Villareal R, Villareal DT, Avioli LV, Civitelli R. Estrogen status and heredity are major determinants of premenopausal bone mass. *J Clin Invest*. 1992 Dec;90(6):2464-71.
  41. Galuska DA, Sowers MR. Menstrual history and bone density in young women. *J Womens Health Gen Based Med*. 1999 Jun;8(5):647-56.
  42. Ruffing JA, Nieves JW, Zion M, Tendy S, Garrett P, Lindsay R, Cosman F. The influence of lifestyle, menstrual function and oral contraceptive use on bone mass and size in female military cadets. *Nutr Metab (Lond)*. 2007;4:17.
  43. Cadogan J, Eastell R, Jones N, Barker ME. Milk intake and bone mineral acquisition in adolescent girls: randomised, controlled intervention trial. *BMJ*. 1997 Nov 15;315(7118):1255-60.
  44. Chan GM, Hoffman K, McMurry M. Effects of dairy products on bone and body composition in pubertal girls. *J Pediatr*. 1995 Apr;126(4):551-6.
  45. Modlesky CM, Majumdar S, Dudley GA. Trabecular bone microarchitecture in female collegiate gymnasts. *Osteoporos Int*. 2008 Jul;19(7):1011-8.
  46. Nickols-Richardson SM, Modlesky CM, O'Connor PJ, Lewis RD. Premenarcheal gymnasts possess higher bone mineral density than controls. *Med Sci Sports Exerc*. 2000 Jan;32(1):63-9.
  47. Heinonen A, Kannus P, Sievänen H, Oja P, Pasanen M, Rinne M, Uusi-Rasi K, Vuori I. Randomised controlled trial of effect of high-impact exercise on selected risk factors for osteoporotic fractures. *Lancet*. 1996 Nov 16;348(9038):1343-7.
  48. Modlesky CM, Majumdar S, Narasimhan A, Dudley GA. Trabecular bone microarchitecture is deteriorated in men with spinal cord injury. *J Bone Miner Res*. 2004 Jan;19(1):48-55.
  49. Slade JM, Bickel CS, Modlesky CM, Majumdar S, Dudley GA. Trabecular bone is more deteriorated in spinal cord injured versus estrogen-free postmenopausal women. *Osteoporos Int*. 2005 Mar;16(3):263-72.
  50. Ingle BM, Hay SM, Bottjer HM, Eastell R. Changes in bone mass and bone turnover following distal forearm fracture. *Osteoporos Int*. 1999;10(5):399-407.
  51. Singer BR, McLaughlan GJ, Robinson CM, Christie J. Epidemiology of fractures in 15,000 adults: the influence of age and gender. *J Bone Joint Surg Br*. 1998 Mar;80(2):243-8.
  52. Cummings SR, Kelsey JL, Nevitt MC, O'Dowd KJ. Epidemiology of osteoporosis and osteoporotic fractures. *Epidemiol Rev*. 1985;7:178-208.
  53. Cummings SR, Black DM, Rubin SM. Lifetime risks of hip, Colles', or vertebral fracture and coronary heart disease among white postmenopausal women. *Arch Intern Med*. 1989 Nov;149(11):2445-8.
  54. Cooper C, Atkinson EJ, Jacobsen SJ, O'Fallon WM, Melton LJ 3rd. Population-based study of survival after osteoporotic fractures. *Am J Epidemiol*. 1993 May 1;137(9):1001-5.
  55. Mallmin H, Ljunghall S, Persson I, Naessén T, Krusemo UB, Bergström R. Fracture of the distal forearm as a forecaster of subsequent hip fracture: a

population-based cohort study with 24 years of follow-up. *Calcif Tissue Int.* 1993 Apr;52(4):269-72.

**56.** Lauritzen JB, Schwarz P, McNair P, Lund B, Transbøl I. Radial and humeral fractures as predictors of subsequent hip, radial or humeral fractures in women, and their seasonal variation. *Osteoporos Int.* 1993 May;3(3):133-7.

**57.** Cuddihy MT, Gabriel SE, Crowson CS, O'Fallon WM, Melton LJ 3rd. Forearm fractures as predictors of subsequent osteoporotic fractures. *Osteoporos Int.* 1999;9(6):469-75.

**58.** Kanis JA, Burlet N, Cooper C, Delmas PD, Reginster JY, Borgstrom F, Rizzoli R; European Society for Clinical and Economic Aspects of Osteoporosis and Osteoarthritis (ESCEO). European guidance for the diagnosis and management of osteoporosis in postmenopausal women. *Osteoporos Int.* 2008 Apr;19(4):399-428.

**59.** Preventive OUS, Task S; U.S. Preventive Services Task Force. Screening for osteoporosis: U.S. preventive services task force recommendation statement. *Ann Intern Med.* 2011 Mar 1;154(5):356-64.

**60.** U.S. Department of Health and Human Services. Bone health and osteoporosis: a report of the surgeon general. Rockville; U.S. Department of Health and Human Services, Office of the Surgeon General; 2004.

**61.** Weycker D, Macarios D, Edelsberg J, Oster G. Compliance with drug therapy for postmenopausal osteoporosis. *Osteoporos Int.* 2006;17(11):1645-52.

**62.** Wade SW, Curtis JR, Yu J, White J, Stolshek BS, Merinar C, Balasubramanian A, Kallich JD, Adams JL, Viswanathan HN. Medication adherence and fracture risk among patients on bisphosphonate therapy in a large United States health plan. *Bone.* 2012 Apr;50(4):870-5.

**63.** Siris ES, Selby PL, Saag KG, Borgström F, Herings RM, Silverman SL. Impact of osteoporosis treatment adherence on fracture rates in North America and Europe. *Am J Med.* 2009 Feb;122(2)(Suppl):S3-13.

**64.** Landfeldt E, Ström O, Robbins S, Borgström F. Adherence to treatment of primary osteoporosis and its association to fractures—the Swedish Adherence Register Analysis (SARA). *Osteoporos Int.* 2012 Feb;23(2):433-43.